Bull Earthquake Eng (2013) 11:455–480
DOI 10.1007/s10518-012-9397-0

ORIGINAL RESEARCH PAPER

Damage potential of near-fault records: sliding displacement against conventional "Intensity Measures"

Evangelia Garini · George Gazetas

Received: 25 April 2012 / Accepted: 22 October 2012 / Published online: 18 November 2012

Abstract The potential of a particular ground accelerogram to inflict damage to asymmetric strongly-inelastic systems is studied in the paper. An idealised analogue, the rigid block with frictional contact on an inclined base, is adopted as the generic representation of such systems. The inclined base (of (a sufficiently steep) angle) is shaken with numerous strong records bearing the effects of forward-directivity and/or fling-step. The accumulated slippage, D, of the block caused by each record is taken as the induced "damage" to the system. The relevance of a variety of 'Intensity Measures' of each accelerogram (ranging from PGA and PGV to Housner's and Arias' Intensities) in predicting this damage, is investigated statistically. It is shown that only a few of these 'Intensity Measures' are reasonably successful and their use could therefore be recommended, but only for statistical inference. A detailed deterministic analysis presented in the paper for one of these successful measures, Arias Intensity, reveals the unacceptably poor predictive power of this measure. Upper-bound curves of slippage provided in closed-form expressions, are an improvement over the state-of-practice Makdisi & Seed diagrams.

Keywords Near-fault motions · Directivity · Fling · Sliding displacement · Intensity measures · Damage potential · Arias Intensity · Housner Intensity · Tohoku earthquake

List of symbols

$A(t)$	Acceleration time-history
$A_{C1} = \alpha_{C1}\mathrm{g}$	Critical (or yielding) acceleration of the block for sliding downward
$A_{C2} = \alpha_{C2}\mathrm{g}$	Critical (or yielding) acceleration of the block upward
A_H	peak value of the base ground acceleration
A_{RMS}	square root of the mean of ground acceleration (see Eq. 5)
ASI	Acceleration Spectrum Intensity (see Eq. 10)
CAV	Cumulative Absolute Velocity (see Eq. 9)

E. Garini · G. Gazetas (✉)
National Technical University of Athens, Athens, Greece
e-mail: gazetas@ath.forthnet.gr

$D(t)$	Sliding displacement time-history
D	Residual (permanent) sliding displacement
D_{RMS}	square root of the mean of ground displacement (see Eq. 7)
I_A	Arias intensity (see Eq. 3)
I_C	Characteristic intensity (see Eq. 8)
I_H	Housner intensity (see Eq. 4)
M	Earthquake magnitude
M_W	Moment earthquake magnitude
P_D	Destructiveness Potential Factor (see Eq. 12)
P_V	Modified Destructiveness Potential Factor
PGA	Peak ground acceleration of ground motion
PGV	Peak ground velocity of ground motion
PGD	Peak ground displacement of ground motion
R_F	Site distance from the fault
R^2	Correlation coefficient
SMA	Sustained Maximum Acceleration
SMV	Sustained Maximum Velocity
T_P	predominant period of ground motion
T_{mean}	mean period of ground motion (see Eq. 13)
$V(t)$	velocity time-history
V_{RMS}	square root of the mean of ground velocity (see Eq. 6)
VSI	Velocity Spectrum Intensity (see Eq. 11)
β	angle of the inclined plane measured from the horizontal
ΔV	maximum velocity step (Bertero et al 1976)
μ	Coulomb's constant coefficient of friction

1 Introduction: asymmetric slippage as an index of potential "Destructiveness"

For geotechnical and structural systems whose deformation involves restoring mechanisms with a dominant linear component, the (damped) elastic response spectra of a particular accelerogram provide an excellent indication of its potential to cause unacceptable amplitudes of deformation in such structures (as a function of their fundamental period). However, for systems with strongly nonlinear and/or inelastic restoring mechanisms, elastic response spectra are often inadequate descriptors of the damage potential. This is particularly so in cases where no elastic component of restoring mechanism is present, such as with systems which rely solely on friction for lateral support. In geotechnical engineering, gravity retaining walls and slopes rely primarily on frictional interfaces (rather than elastic restraint) for resistance to seismic shaking. But even structures that are designed to respond mainly in the inelastic region with ductility levels of 3 or more have restoring force-displacement relationships which resemble those of frictional mechanisms.

Such geotechnical applications include the seismic deformation analysis of earth dams and embankments (Seed and Martin 1966; Ambraseys and Sarma 1967; Sarma 1975, 1981; Franklin and Chang 1977; Makdisi and Seed 1978; Lin and Whitman 1983; Constantinou et al. 1984; Constantinou and Gazetas 1987; Yegian et al. 1991; Sawada et al. 1993; Gazetas et al. 1981; Gazetas and Uddin 1994; Kramer and Smith 1997); the displacements associated with landslides (Jibson 1994; Harp and Jibson 1995); yielding displacements of gravity retaining walls (Richards and Elms 1979; Stamatopoulos et al. 2006); the seismic deformation of landfills with geosynthetic liners (Yegian et al. 1998; Bray and Rathje 1998); the

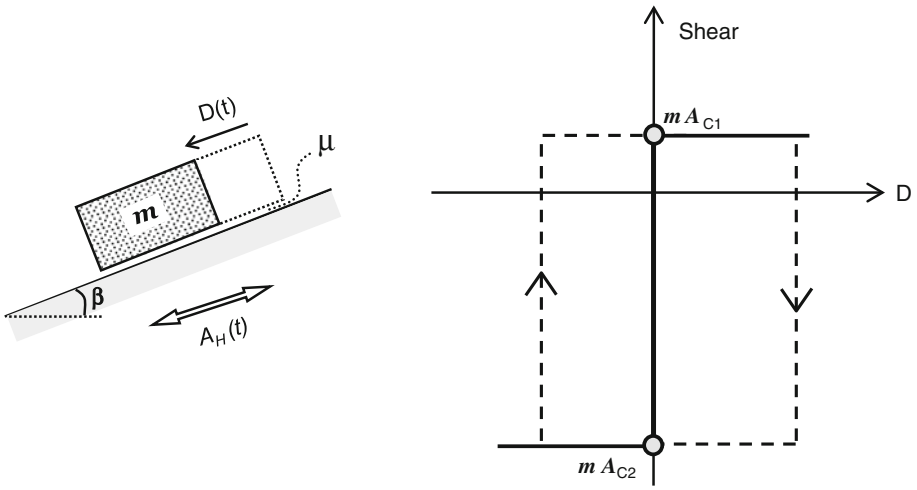

Fig. 1 Schematic representation of the 'Newmark' sliding-block analogue and the interface shear force ("friction") as a function of slip displacement

seismic settlement of surface foundations (Richards et al. 1993). Several other generalized applications have also appeared (examples: Ambraseys and Srbulov 1994; Stamatopoulos 1996; Makris and Chang 2000; Ling 2001; Kramer and Lindwall 2002; Wartman et al. 2003; Lagomarsino and Giovinazzi 2006).

An abstraction has been inspired by the above applications. To assess the potential of a particular accelerogram to inflict large irrecoverable deformation on highly inelastic systems, the idealized system of a rigid block resting on an inclined base is subjected to this accelerogram. *The amount of the incurring downhill slippage is taken as the inflicted damage by this motion.* Called "Newmark sliding" in the geotechnical literature [after the introduction by Newmark (1965) of the slippage of a wedge from an embankment slope as a measure of its seismic performance] this particular system is thought of as an analogue of actual inelastic systems.

The asymmetric sliding system is characterized by an ideally rigid-plastic relationship of restoring force versus displacement, in accordance with Coulomb's friction law, as sketched in Fig. 1. The supporting base is subjected to the particular ground motion under investigation, and the size of the resulting slippage, serves as the measure of damage that this motion can inflict on the inelastic systems—the "destructiveness potential" (or as usually called in the literature the "intensity measure") of the particular motion.

The maximum resistance ("strength") of the system is controlled by the coefficient of friction of the interface, μ. By letting μ vary parametrically for a given ground motion, we obtain the "sliding" spectra. It could be argued that such spectra offer a more informative picture of inelastic response (and damage) than the elastic response spectra or even the constant-ductility spectra (obtained by the normative procedure of down-scaling the elastic spectra as a function of ductility)—see Bertero (1976) and Bertero et al. (1978) for an early recognition of the inadequacy of the latter.

2 Fundamentals of sliding on an inclined base

The analysis of the behavior of a block on an inclined base subjected to motion A(t) parallel to the plane is obtained from elementary rigid body kinematics along with Newton's second law

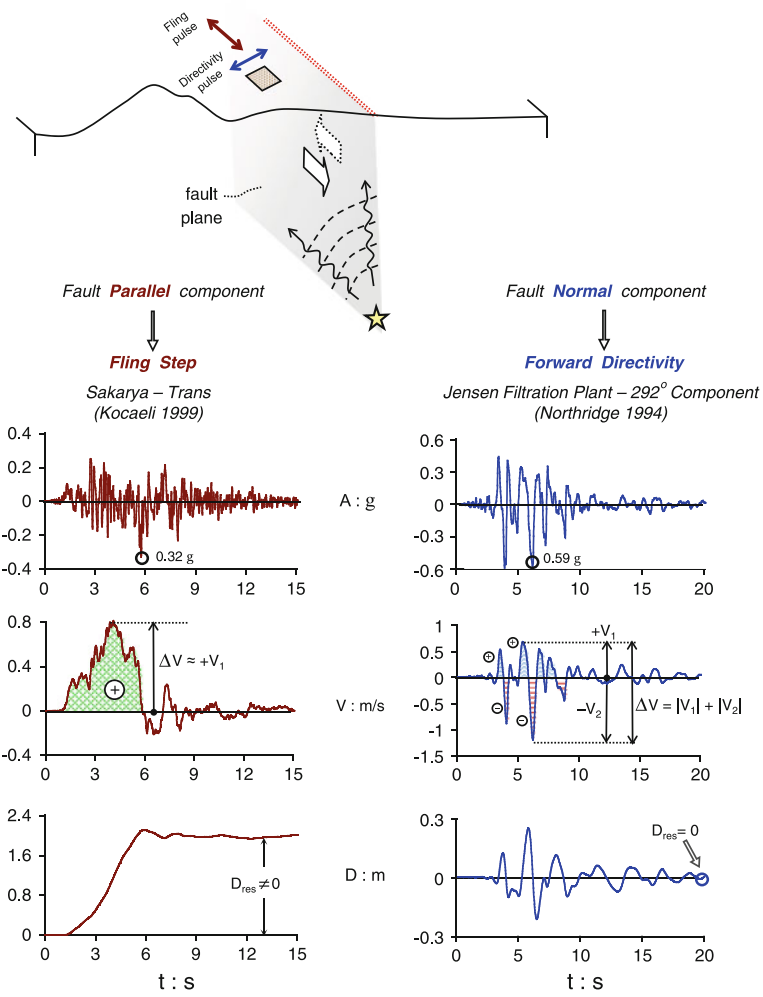

Fig. 2 Schematic explanation of the 'fling-step' and 'forward-directivity' phenomena as reflected in two characteristic records: the fling affected Sakarya motion (*left*) and the directivity affected Jensen Filtration Plant record (*right*)

of motion (Fig. 1). The critical values of acceleration which must be exceeded for slippage to be initiated downhill or uphill are respectively:

$$A_{C1} = (\mu\cos\beta - \sin\beta)g \tag{1a}$$

$$A_{C2} = (\mu\cos\beta + \sin\beta)g \tag{1b}$$

in which μ = the (constant) coefficient of friction; and β = the angle of the inclined plane. Even for small inclination angles, for example 5° and for $\mu = 0.1$, the uphill yielding acceleration $A_{C2} = 0.186\,g >> A_{C1} = 0.012\,g$. As a result, sliding takes place only downhill (hence the name "asymmetric"). Herein the inclination angle, β, is equal to 25° representative of a steep sloping plane.

Table 1 List of significant earthquake records bearing the effects of 'directivity' and 'fling', utilized as excitations in this study

Earthquake, magnitude	Record name	PGA (g)	PGV (m/s)	PGD (m)
	Fukiai	0.763	1.232	0.134
	JMA-0°	0.830	0.810	0.177
	JMA-90°	0.599	0.761	0.199
Kobe—Japan,	Nishi Akash-0°	0.509	0.357	0.091
(16 January 1995)	Nishi Akash-90°	0.503	0.356	0.109
$M_W = 7.0$	Shin Kob-NS	0.422	0.688	0.169
$M_{JMA} = 7.2$	Takarazuka-0°	0.693	0.682	0.274
	Takarazuka-90°	0.694	0.853	0.167
	Takatori-0°	0.611	1.272	0.358
	Takatori-90°	0.616	1.207	0.328
	No 4–140°	0.485	0.374	0.202
	No 4–230°	0.360	0.766	0.590
	No 5–140°	0.519	0.469	0.353
Imperial Valley—California,	No 5–230°	0.379	0.905	0.630
(15 October 1979)	No 6–140°	0.410	0.649	0.276
$M_W = 6.8$	No 6–230°	0.439	1.098	0.658
	No 7–140°	0.338	0.476	0.246
	No 7–230°	0.463	1.093	0.447
	No 9 Differential Array-270°	0.352	0.712	0.458
	No 9 Differential Array-360°	0.480	0.408	0.140
Landers—California,	Lucerne-0°	0.785	0.319	0.164
(28 June 1992)	Lucerne-275◦	0.721	0.976	0.703
$M_W = 7.3$	Joshua Tree-0°	0.274	0.275	0.098
	Joshua Tree-90°	0.284	0.432	0.145
San Fernando—California,	Pacoima Dam-164°	1.226	1.124	0.361
(9 February 1971)		1.160	0.536	0.111
$M_S = 6.7$	Pacoima Dam-254°			
Erzincan—Turkey,	Erzincan (Station 95)-EW	0.496	0.643	0.236
(13 March 1992)		0.515	0.839	0.312
$M_S = 6.9$	Erzincan (Station 95)-NS			
Loma Prieta—California,	Los Gatos Presentation Center-0°	0.563	0.948	0.411
(17 October 1989)	Los Gatos Presentation Center-90°	0.605	0.510	0.115
$M_S = 7.1$	Saratoga Aloha Avenue-0°	0.512	0.412	0.162
$M_w = 6.8$	Saratoga Aloha Avenue-90 °	0.324	0.426	0.275
Gazli—USSR,	Karakyr-0°	0.608	0.654	0.253
(17 May 1946)	Karakyr-90°	0.718	0.716	0.237
$M_S = 7.0$	Jensen Filtration Plant-22°	0.424	0.873	0.265
	Jensen Filtration Plant-292 °	0.592	1.201	0.249
	L.A. Dam-64°	0.511	0.637	0.211
	L.A. Dam-334°	0.348	0.508	0.151

Table 1 continued

Earthquake, magnitude	Record name	PGA (g)	PGV (m/s)	PGD (m)
	Newhall Firestation-90°	0.583	0.524	0.126
	Newhall Firestation-360°	0.589	0.753	0.182
	Pacoima Dam (downstream)-175°	0.415	0.456	0.050
	Pacoima Dam (downstream)-265°	0.434	0.313	0.048
Northridge 1994—California,	Pacoima Kagel Canyon-90°	0.301	0.379	0.095
(17 January 1994)	Pacoima Kagel Canyon-360°	0.432	0.452	0.069
$M_w = 6.8$	Rinaldi-228°	0.837	1.485	0.261
	Rinaldi-318°	0.472	0.627	0.166
	Santa Monica City Hall-90°	0.883	0.403	0.102
	Santa Monica City Hall-360°	0.369	0.232	0.059
	Sepulveda VA-270°	0.753	0.848	0.186
	Sepulveda VA-360°	0.939	0.766	0.149
	Simi Valley Katherine Rd-0°	0.877	0.409	0.053
	Simi Valley Katherine Rd-90°	0.640	0.378	0.051
	Sylmar Hospital-90°	0.604	0.744	0.165
	Sylmar Hospital-360°	0.843	1.027	0.256
	TCU 052-EW	0.350	1.743	4.659
	TCU 052-NS	0.437	2.186	7.319
	TCU 065-EW	0.450	1.298	1.820
	TCU 065-NS	0.554	0.876	1.254
	TCU 067-EW	0.487	0.973	1.953
	TCU 067-NS	0.311	0.536	0.849
	TCU 068-EW	0.491	2.733	7.149
Chi–Chi Taiwan,	TCU 068-NS	0.353	2.892	8.911
(20 September 1999)	TCU 075-EW	0.324	1.143	1.692
$M_w = 7.5$	TCU 075-NS	0.254	0.360	0.414
	TCU 076-EW	0.335	0.706	1.223
	TCU 076-NS	0.416	0.617	0.662
	TCU 080-EW	0.968	1.076	0.186
	TCU 080-NS	0.902	1.025	0.340
	TCU 084-EW	0.986	0.923	0.910
	TCU 084-NS	0.419	0.486	0.966
	TCU 102-EW	0.297	0.870	1.478
	TCU 102-NS	0.168	0.705	1.062
	Duzce-180°	0.312	0.474	0.285
Kocaeli—Turkey,	Duzce-270°	0.358	0.464	0.176
(17 August 1999)	Sakarya-EW	0.330	0.814	2.110
$M_w = 7.4$	Yarimca-60°	0.231	0.906	1.981
$M_S = 7.8$	Yarimca-330°	0.322	0.867	1.493
Tabas—Iran,	Tabas-LN	0.836	0.978	0.387
(16 September 1978)				
$M_S = 7.4$	Tabas-TR	0.852	1.212	0.951

Table 1 continued

Earthquake, magnitude	Record name	PGA (g)	PGV (m/s)	PGD (m)
	National Geographical Institute-180°	0.392	0.566	0.206
San Salvador-El Salvador,	National Geographical Institute-270°	0.524	0.753	0.116
(10 October 1986)	Geotechnical Investigation Center-90°	0.681	0.793	0.119
$M_S = 5.4$	Geotechnical Investigation Center-180°	0.412	0.602	0.201
$M_w = 5.6$	Institute of Urban Construction-90°	0.380	0.441	0.173
	Institute of Urban Construction-180°	0.668	0.595	0.112
	Bolu-0°	0.728	0.564	0.231
Duzce-Turkey,	Bolu-90°	0.822	0.621	0.135
(12 November 1999)				
$M_S = 7.5$	Duzce-180°	0.348	0.600	0.421
$M_w = 7.2$	Duzce-270°	0.535	0.835	0.516

Whenever the base acceleration exceeds A_{C1} (or, rarely, A_{C2}) slippage of the block takes place with respect to the base. This slippage lasts only momentarily, thanks to the transient nature of earthquake shaking; it terminates as soon as the velocities of the base and the block equalize. And the process continues until the motions of both the block and the base eventually terminate.

3 Description of available "Damage Potential Indices" (DPI)

Earthquake records contain information on the seismic intensity and potential destructiveness of ground shaking. Numerous parameters of a ground motion have been proposed over the years to serve as indices of the potential of this motion to inflict damage to structural and geotechnical systems. They are often called "Intensity Measures" but we prefer here the term "Damage Potential Indices" (DPI). Their use is in response to the need for a rapid assessment of such potential of recorded motions, before a complete analysis can be made. Moreover, predicting a DPI from a pertinent attenuation relation:

$$\mathrm{DPI} = \mathrm{f}\,(\mathrm{M_W}, \mathrm{R_F}, \text{site conditions}) \tag{2}$$

allows a direct assessment of the earthquake threat; where M_W is the moment magnitude of an earthquake, and R_F is the distance from the fault.

Several such DPI are being tested here against the magnitude of accumulated slippage, D, induced by a ground motion. Detailed definitions of the tested indices are given in the following:

- The peak ground motion's values of acceleration PGA, velocity PGV, and displacement PGD.
- Arias Intensity, I_A, is proportional to the integral of the squared acceleration A(t) time history (Arias 1970):

$$\mathrm{I_A} = \frac{\pi}{2g}\int \mathrm{A}^2(t)dt \tag{3}$$

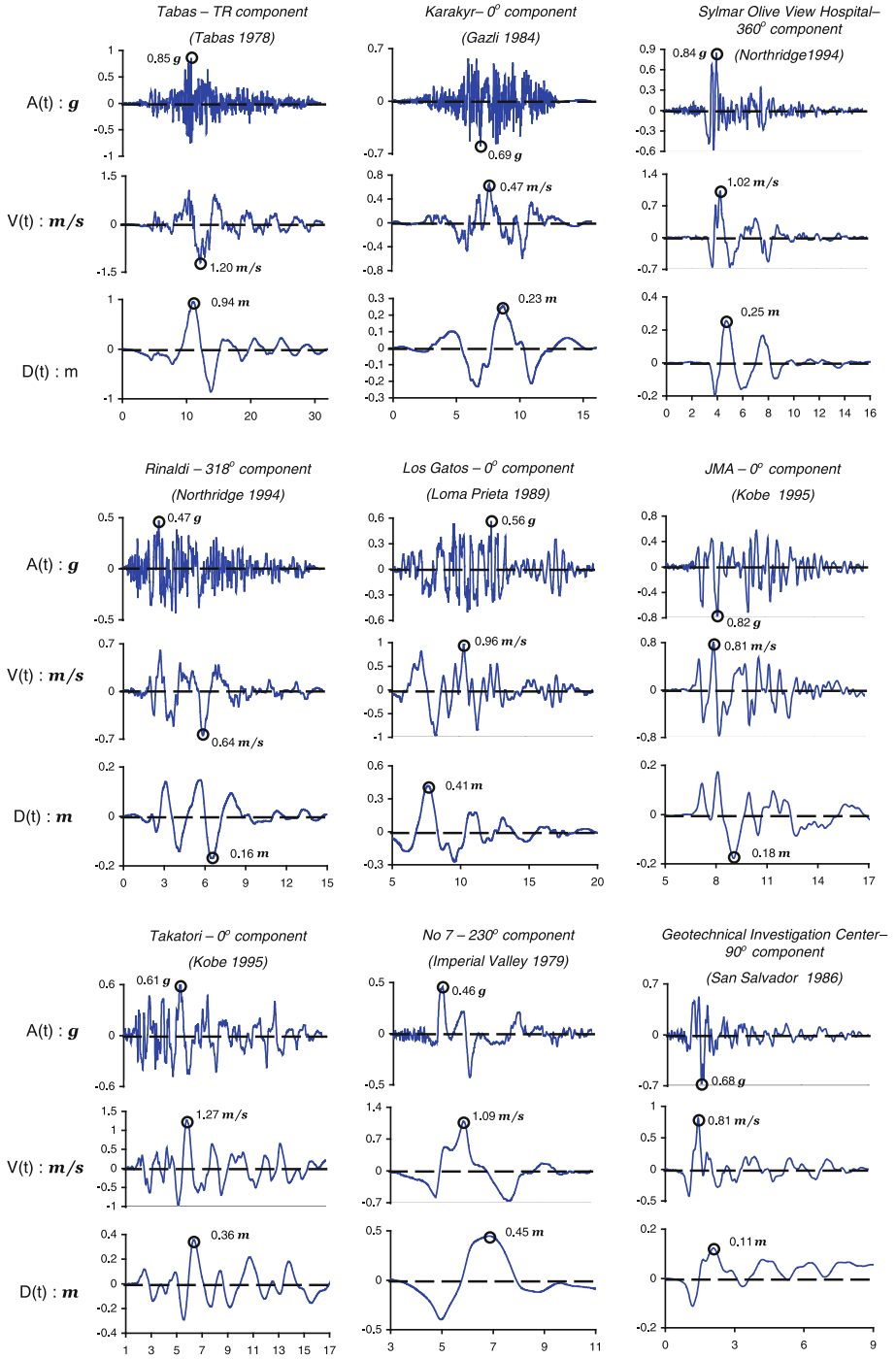

Fig. 3 Selection of records with prominent directivity acceleration pulses, employed as excitations studied in this paper

- Housner Intensity, I_H, is the integral of the pseudo-velocity response spectrum over the period range [0.1 s, 2.5 s] (Housner 1952):

$$I_H = \int_{0.1}^{2.5} PS_V(T, \xi = 5\,\%)dT \tag{4}$$

- RMS acceleration, A_{RMS}, is the square root of the mean of the acceleration A(t):

$$A_{RMS} = \sqrt{\frac{\int A^2(t)dt}{T_D}} \tag{5}$$

in which T_D = the duration of the record.

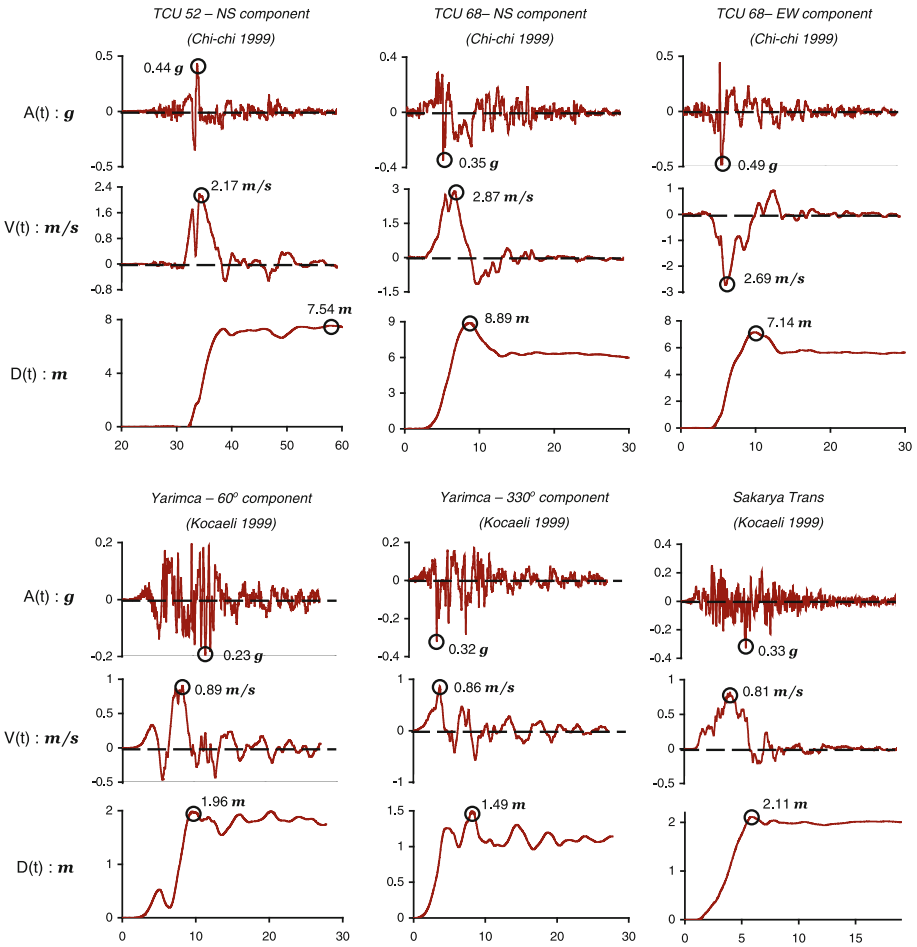

Fig. 4 Selection of records strongly affected by fling, employed as excitations studied in this paper

- RMS velocity, V_{RMS}, is the root mean square of the velocity record V(t):

$$V_{RMS} = \sqrt{\frac{\int V^2(t)dt}{T_D}} \tag{6}$$

- RMS displacement, D_{RMS}, is the root mean square of the displacement record D(t):

$$D_{RMS} = \sqrt{\frac{\int D^2(t)dt}{T_D}} \tag{7}$$

- Characteristic Intensity, I_C, is defined as:

$$I_C = (A_{RMS})^{3/2}\sqrt{T_D} \tag{8}$$

- Cumulative Absolute Velocity, CAV, is defines as:

$$CAV = \sum_{i=1}^{N} H(PGA_i - A_{\min}) \int_{t_i}^{t_{i+1}} |A(t)|dt \tag{9}$$

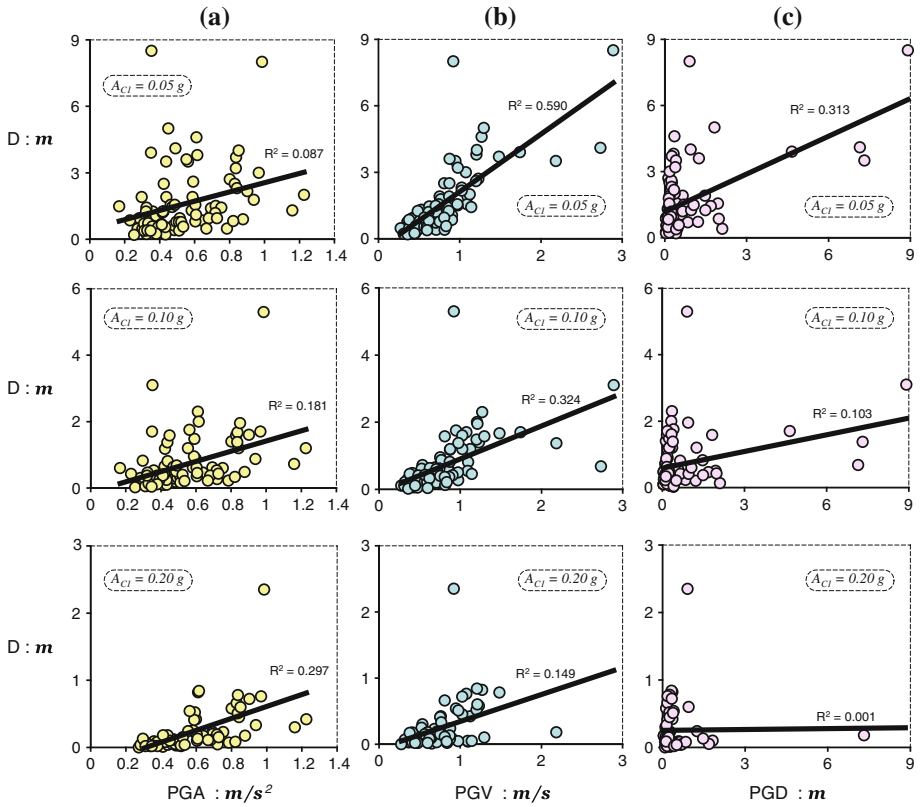

Fig. 5 Slippage, *D*, correlated with the most widely used ground motion "Intensity" parameters: **(a)** peak ground acceleration, **(b)** peak ground velocity, and **(c)** peak ground displacement

where N is the number of 1-second time windows in the time series, PGA_i is the PGA (normalised by g) during time window i, t_i is the start time of time window i, A_{min} is an acceleration threshold (user-defined, usually taken as 0.025 g) to exclude low amplitude motions contributing to the sum, and H(x) is the Heaviside step function (unity for x > 0, zero otherwise).

- Sustained Maximum Acceleration, SMA, is the third highest absolute peak in the acceleration time history (Nuttli 1979).
- Sustained Maximum Velocity, SMV, is the third highest absolute peak in the velocity time history (Nuttli 1979).
- Acceleration Spectrum Intensity, ASI, is calculated from the spectral acceleration (Von Thun et al. 1988):

$$ASI = \int_{0.1}^{0.5} S_A\,(5\,\%, \mathrm{T})\,d\mathrm{T} \tag{10}$$

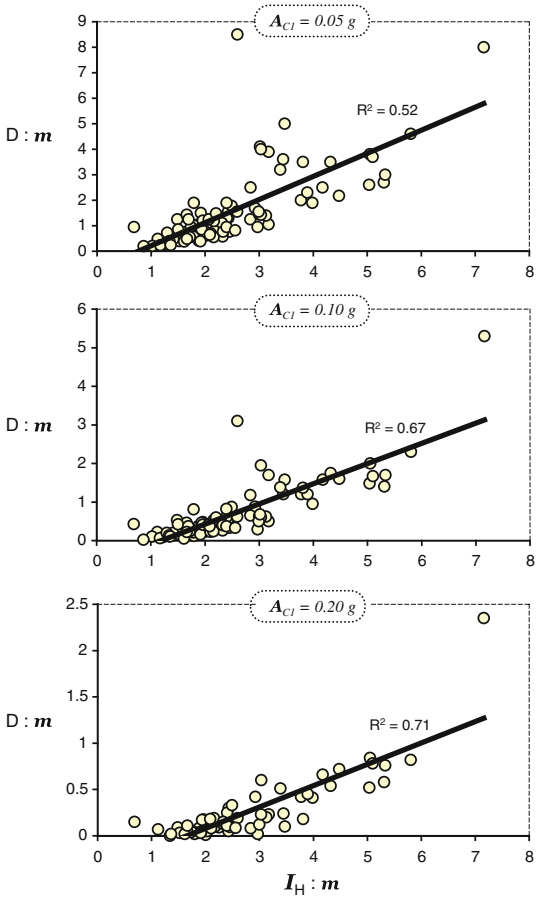

Fig. 6 Correlation between the Housner Intensity, I_H, of the records studied herein and the triggered sliding displacement, *D*, for three values of critical acceleration A_{C1}

- Velocity Spectrum Intensity, VSI, is calculated from the spectral velocity (Von Thun et al. 1988):

$$VSI = \int_{0.1}^{2.5} S_V\,(5\,\%, \mathrm{T})\,d\mathrm{T} \tag{11}$$

Notice that the velocity spectrum intensity (VSI) and Housner intensity (I_H) are almost identical parameters with the only difference being that Housner's intensity is calculated from the pseudo velocity spectrum whereas VSI is based on the true velocity spectrum.

- Spectral Displacement, $S_{D,T}$, at values of natural period T = 1, 2, 3, 4 s.
- Acceleration parameter A_{95} is the level of acceleration which contains up to 95 % of the Arias Intensity (Sarma and Yang 1987).
- Destructiveness Potential Factor, P_D, (Araya and Saragoni 1984; Crespellani et al. 1998) is the ratio between the Arias Intensity I_A and the square of the number of zero crossings per second (ν_0) of the accelerogram:

$$P_D = \frac{I_A}{\nu_0^2} = \frac{\pi}{2g}\frac{\int A^2(t)dt}{\nu_0^2} \tag{12}$$

- Modified Destructiveness Potential Factor, P_V, is the ratio between the Arias Intensity I_A and the square of the number of zero crossings per second ν_1 only in the "significant"

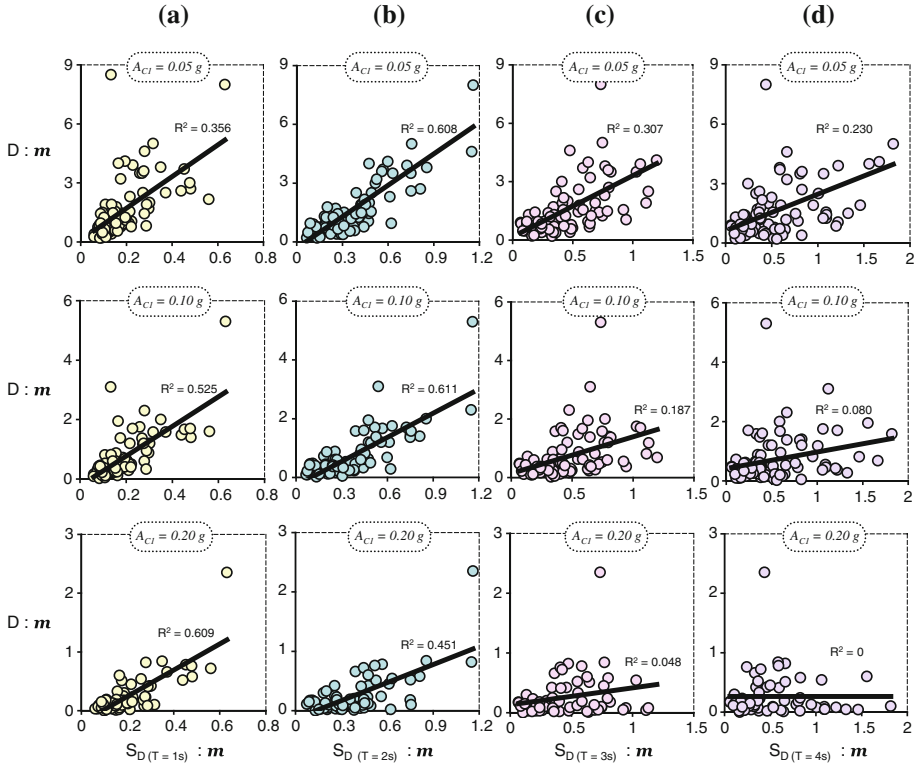

Fig. 7 Correlation of slippage, *D*, with spectral displacement S_D values of each excitation at four different periods: **(a)** for T = 1 s, **(b)** for T = 2 s, **(c)** for T = 3 s, and **(d)** for T = 4 s

region of the accelerogram. We define as "significant" the part of record that includes all the long-duration directivity and fling acceleration pulses. Note that this is not a completely objectively-determined index, because the directivity and fling sections can not be determined unequivocally.

Some additional parameters are often used as indices of "destructiveness" but in combination with other parameters; they include: (a) the Predominant Period, T_P, which is estimated using the 5% damped acceleration response spectrum at its maximum (as long as $T_P > 0.20$ s), and (b) the Mean Period, T_{mean}, which is obtained from the Fourier amplitude spectrum as:

$$T_{mean} = \frac{\sum \left(\frac{C_i^2}{f_i} \right)}{\sum C_i^2} \tag{13}$$

where C_i is the Fourier amplitude for each frequency f_i within the range 0.25–20 Hz.

4 The near-fault phenomena in earthquake records: "Directivity" and "Fling"

In the neighbourhood of a rupturing seismic fault ground shaking may be affected by wave propagation effects known as "forward directivity" and by tectonic deformation producing

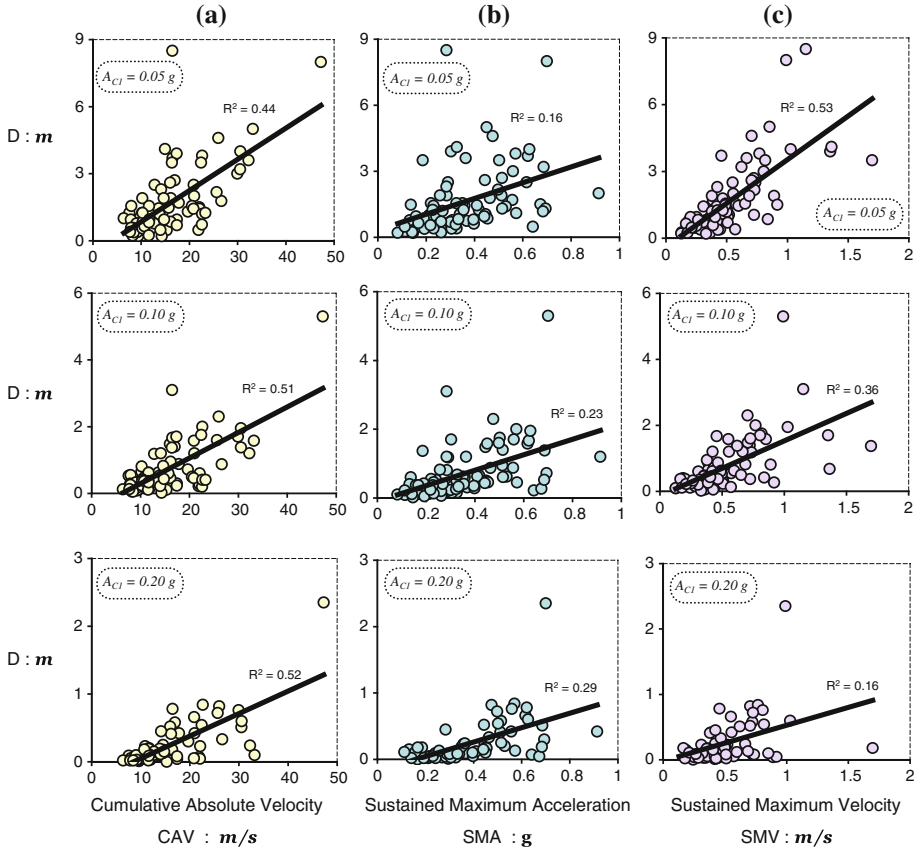

Fig. 8 Slippage, *D*, as a function of : **(a)** the cumulative absolute velocity, **(b)** the sustained maximum acceleration, and **(c)** the sustained maximum velocity

a permanent ground offset known as "fling-step". The former effect is the outcome of the coherent arrival of seismic waves emitted from a seismogenetic fault when its rupturing propagates towards the site. It manifests itself with a single long–duration and high–amplitude pulse occurring near the beginning of shaking, and oriented perpendicularly to the fault (Somerville et al. 1997; Somerville 2000). The fling-step effect is the outcome of the tectonic permanent deformation of the earth in the proximity of the fault. It manifests itself in records exhibiting a substantial residual displacement, oriented parallel to the fault strike with "strike-slip" earthquakes and perpendicular to the fault strike with purely dip-slip ("normal" or "thrust") earthquakes (Abrahamson 2000, 2001).

Figure 2 shows a sketch of a strike-slip event, portraying the idealized "signatures" of the two phenomena on the fault-normal and fault-parallel components of the displacement record. Two remarkable accelerograms are depicted in Fig. 2, Sakarya (from Kocaeli 1999) and Jensen Filtration Plant (from Northridge 1994). They exhibit fling-step and forward directivity effects, respectively. The velocity time history of Sakarya contains a large pulse (0.8 m/s) of huge duration (4 s), which is consistent with the permanent ground offset of about 2 m that can be seen in the derived displacement record, and which has actually been observed in the field (with geodetic measurements). The derived velocity time history of Jensen contains several cycles with a devastating maximum velocity step $\Delta V \simeq 1.8$ m/s. The destructive capacity of such a velocity increment has been first elaborated by Bertero (1976) in relation to the failure of Olive View Hospital in the 1971 San Fernando earthquake.

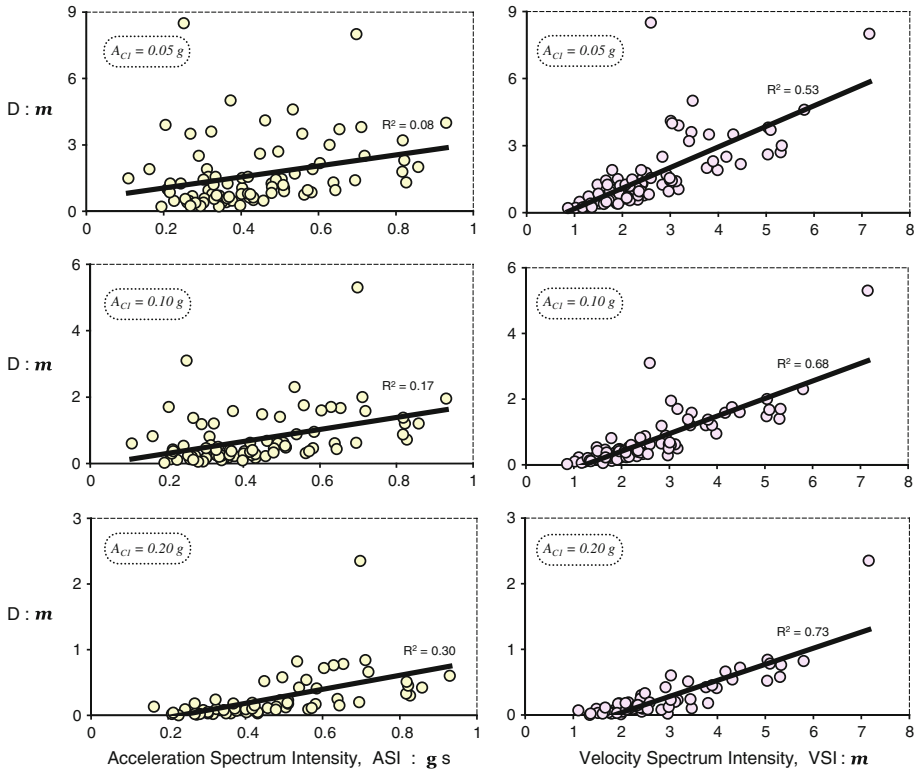

Fig. 9 Correlation of slippage, D, with the acceleration and velocity spectrum intensities

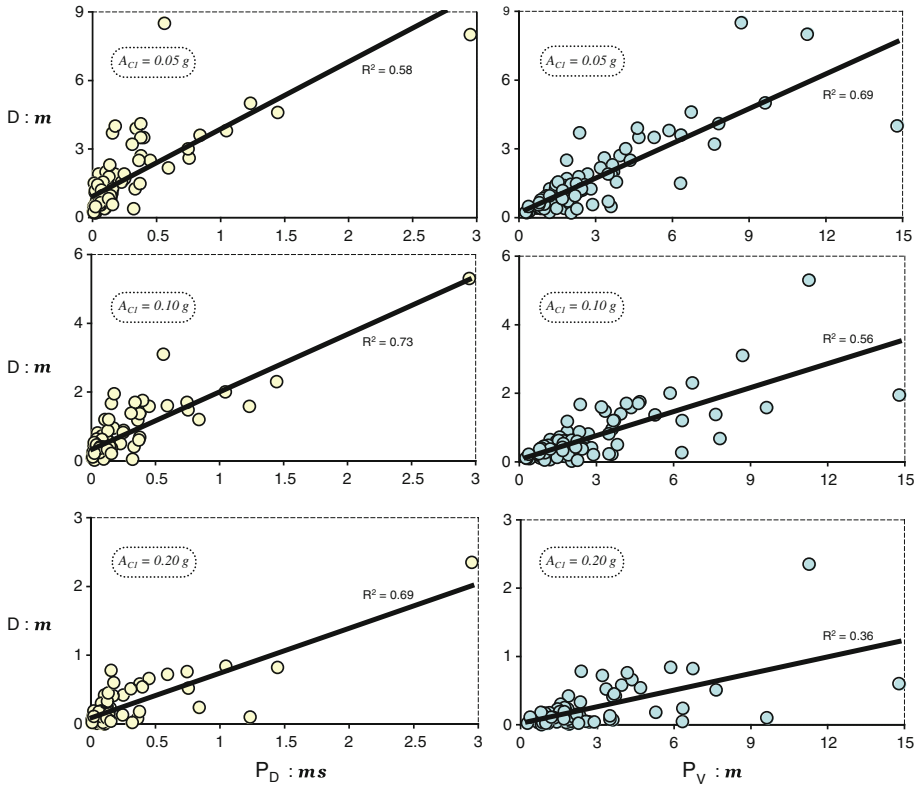

Fig. 10 Correlation of slippage *D*, with the potential destructiveness factor, P_D, and "velocity modified" potential destructiveness factor, P_V

Research efforts on assessing the potential of directivity and fling pulses to inflict damage to a variety of geotechnical and structural systems (the latter falling mostly in the realm of elastic or elastoplastic response) have been reported by : Singh (1985), Hall et al. (1995), Kramer and Smith (1997), Iwan et al. (2000), Sasani and Bertero (2000), Makris and Roussos (2000), Alavi and Krawinkler (2000), Pavlou and Constantinou (2004), Shen et al. (2004), Mavroeidis et al. (2004), Pitilakis (2004), Xu et al. (2006), Changhai et al. (2007). Most of these studies refer to "directivity" effects, with much less effort on the "destructiveness" of ground motions containing 'fling-step' pulses (e.g. Gazetas et al. 2009; Seyedi et al. 2007). This is not surprising because the phenomenon has been clearly identified and distinguished from other phenomena after the Kocaeli and Chi–chi earthquakes of 1999 (Abrahamson 2001; Hisada and Bielak 2003).

One of the significant conclusions reached by Bertero (1976), Bertero et al. (1978) in his pioneering work was that:

> The types of excitation that induce the maximum response in elastic and non-elastic systems are fundamentally different and hence one can not derive the maximum non-elastic response from the corresponding elastic one (Bertero 1976).

In other words, a ground motion with severe elastic response spectrum can be very benign to a strongly inelastic system. Hence the selection of the rigid–plastic constant–friction

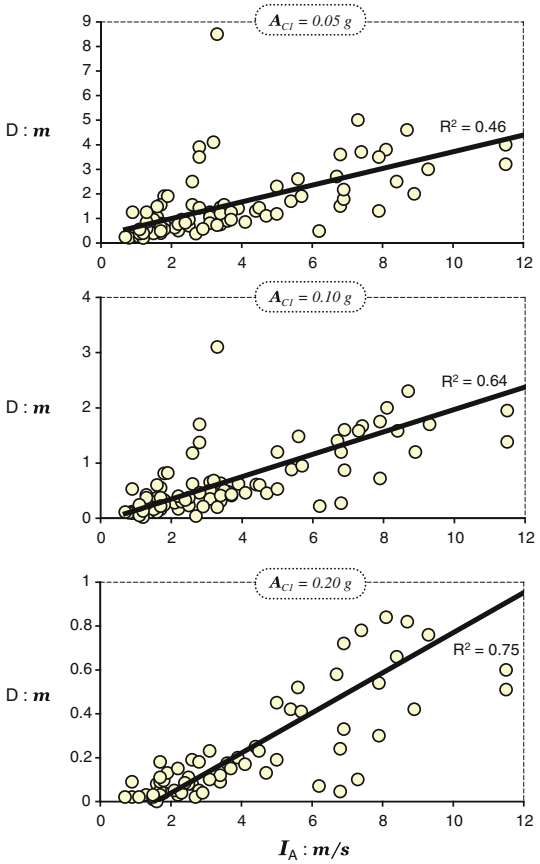

Fig. 11 Correlation between the Arias Intensity, I_A, of the records utilized as excitation and the triggered sliding displacement, D

system as representative of extremely–inelastic behaviour. Indeed, earlier work by the authors (Garini et al. 2011) has shown that such systems are far more sensitive than the purely linear elastic systems (the other extreme of reality) to the peculiarity of near-fault ground shaking. Testing every DPI for each accelerogram against the "damage" (i.e., slippage) computed for such a system excited by this particular accelerogram, is the main goal of this paper (see also Garini and Gazetas 2012). Our emphasis is on the asymmetric sliding, which is more relevant to geotechnical systems, but some attention is given to symmetric sliding (on horizontal base) as well.

4.1 Ground motions utilized in this study

A large number (99) of recorded motions are employed for this testing. The selection covers the records of the last 30 years bearing more-or-less clear near-fault characteristics: directivity and fling effects. Table 1 lists these records along with their PGA, PGV and PGD values. Each accelerogram is imposed as based excitation twice: (i) with its recorded sign ("normal" polarity) and (ii) with opposite sign ("reverse" polarity).

Figures 3 and 4 portray fifteen of the most significant records used in our analyses, in terms of A(t), V(t), D(t).

Table 2 Correlation index, R, between asymmetric sliding response, D, and seismic indices of destructiveness, covering the parametric range of our study

Correlation Index, R	$A_{C1} = 0.05\,g$	$A_{C1} = 0.10\,g$	$A_{C1} = 0.20\,g$
Peak Ground Acceleration, *PGA*	0.09	0.18	0.29
Peak Ground Velocity, *PGV*	0.59	0.32	0.15
Peak Ground Displacement, *PGD*	0.31	0.10	0.001
Arias Intensity, I_A	0.46	0.64	0.75
Destructiveness Potential Factor, P_D	0.58	0.73	0.69
Modified Destructiveness Potential Factor, P_V	0.69	0.56	0.36
Housner Intensity, I_H	0.52	0.67	0.71
RMS Acceleration, A_{RMS}	0.23	0.25	0.24
RMS Velocity, V_{RMS}	0.54	0.26	0.12
RMS Displacement, D_{RMS}	0.07	0.03	0.004
Spectral Displacement at Period of 1 s, $S_{D/(T=1)}$	0.36	0.53	0.61
Spectral Displacement at Period of 2 s, $S_{D/(T=2)}$	0.61	0.61	0.45
Spectral Displacement at Period of 3 s, $S_{D/(T=3)}$	0.31	0.19	0.05
Spectral Displacement at Period of 4 s, $S_{D/(T=4)}$	0.23	0.08	0
Characteristic Intensity, I_C	0.39	0.51	0.55
Cumulative Absolute Velocity, CAV	0.44	0.51	0.52
Sustained Maximum Acceleration, SMA	0.16	0.23	0.29
Sustained Maximum Velocity, SMV	0.53	0.36	0.16
Acceleration Spectrum Intensity, ASI	0.08	0.17	0.30
Velocity Spectrum Intensity, VSI	0.53	0.68	0.73
Acceleration Parameter, A_{95}	0.11	0.19	0.27
Predominant Period, T_P	0.17	0.15	0.14
Mean Period, T_{mean}	0.15	0.07	0.002

5 Results: DPI versus slippage

Figures 5, 6, 7, 8, 9, 10,11 present the correlation between each DPI and the sliding block displacement, D, triggered by each ground motion (the latter applied to the 25° inclined base). Table 2 summarises the results in terms of the correlation coefficients for all the examined DPIs. Several conclusions emerge:

(i) In general, most of the DPIs perform poorly, and some very poorly—they are inadequate descriptors of a motion's severity.
(ii) Most of the acceleration-based indices (PGA, A_{RMS}, I_C, ASI, SMA) are also rather deficient descriptors of slippage.
(iii) By contrast, two of the velocity-based indices (Housner's I_H, and VSI) correlate fairly well with slippage.
(iv) The spectral displacement at the period of 2 s, $S_{D(T=2)}$, the "destructiveness potential factor", P_D, and its modified version, P_V, are moderately good predictors of damage (i.e., magnitude of the sliding response). The difference between P_V and P_D is that the former is best for strongly-inelastic response ($A_{C1} = 0.05$ g) and its performance deteriorates with increasing A_{C1}, whereas the index P_D is somewhat better at larger A_{C1} values.

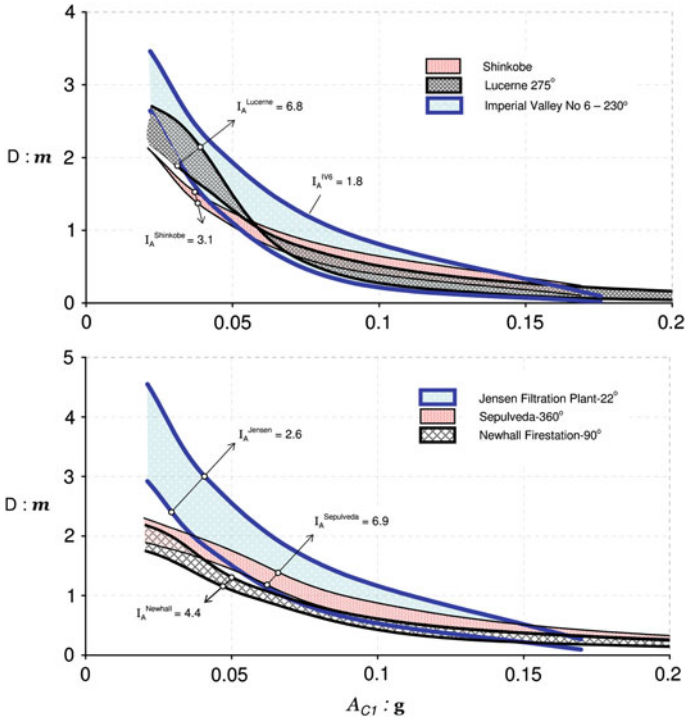

Fig. 12 Induced slippage versus critical acceleration for two groups of records. Each excitation is imposed with both polarities and labeled with its (single) Arias Intensity value

(v) Arias', I_A, intensity correlates rather satisfactorily with slippage, especially as the yield acceleration A_{C1} increases. But let us examine its performance in a more deterministic fashion.

5.1 Arias intensity versus symmetric and asymmetric sliding of an individual record

In the search for reliable indexes of "destructiveness" of ground motions, i.e., for motion parameters indicative of the *severity* of a particular shaking, the question is: severity for which system? Clearly, as Bertero (1976) had shown, what is a severe motion for an elastic system may be a very weak motion for an inelastic system. And vice-versa. The system in this paper has been the strongly-inelastic and asymmetric system of a block driven solely by Coulomb friction on inclined plane. With an excitation containing several cycles having (local) peak accelerations exceeding A_{C1}, the slippage from each such cycle accumulates. Thus a long-duration motion, having many substantial cycles, is likely to give large (total) slippage; the Arias intensity of such a motion is also likely to be large—hence the rather satisfactory statistical correlation between D and I_A (Fig. 11). But other characteristics of a motion, most notably the presence of long-duration acceleration pulses, tend to produce a rather negative correlation.

Thus the question: from the fairly satisfactory statistical performance of I_A could we conclude that this index can be used as a decent predictor of "destructiveness" of a particular ground motion? And in other words, can we compare the potential of two motions to inflict damage from their I_A values? For an answer to these questions, an attempt is made here to

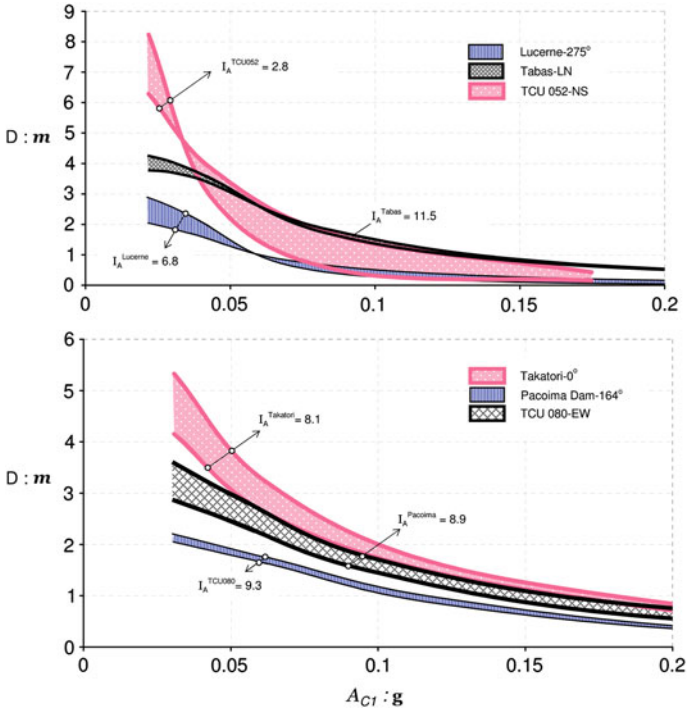

Fig. 13 Sliding displacement versus critical acceleration for two different groups of records. Ground accelerations imposed with both polarities. Notice that as Arias Intensity increases, the induced slippage does not necessarily increases

correlate in a more detailed deterministic way the I_A of some severe near-fault motions with the permanent slip D they cause to a sliding block. To this end, Figs. 12, 13, 14 display the relation between slippage D as a function of the yield acceleration A_{C1}. No scaling or any other modification to the ground motions was made. What appears as scatter in the results of each record, arises solely from the change in polarity (+ or − direction) of each specific record. The computed Arias Intensity of each motion is written directly on the relevant pair of curves.

Evidently, the answer to the above questions is negative: the value of I_A of a specific record does not tell much about the damage (slip) that this record can inflict. In almost all six plots of Figs. 12, 13, 14, the largest D is caused by the motions with the smallest I_A—a negative correlation (at least for the small values $A_{C1} \leq 0.05$ g). Particularly impressive is the top plot of Fig. 14, which illustrates the sliding response of three records of the Chi-chi earthquake. For very small values of A_{C1} (<0.05 g) "damage" from the TCU-084 record, despite its huge value $I_A = 19.5$ m/s, is smaller than that caused by TCU-068, with the very modest $I_A = 3.3$ m/s. Perhaps most remarkable is the vast difference in slippage induced by the single TCU-068 record when imposed with its two different polarities (+ or −).

For another severe test of Arias Intensity (Figs. 15, 16) two long-duration records from the 2011 Tohoku earthquake (the FKS 017 and TCG 014 records) are contrasted with one of the most notorious records from the 1995 Kobe earthquake (the Takatori record). These three records excite both a horizontal and an inclined sliding system—thus allowing a glimpse on the role of slip accumulation. Figure 15 plots on the same scale the three accelerograms and their response spectra. All three records have similar PGA (close to 0.65 g) but the total

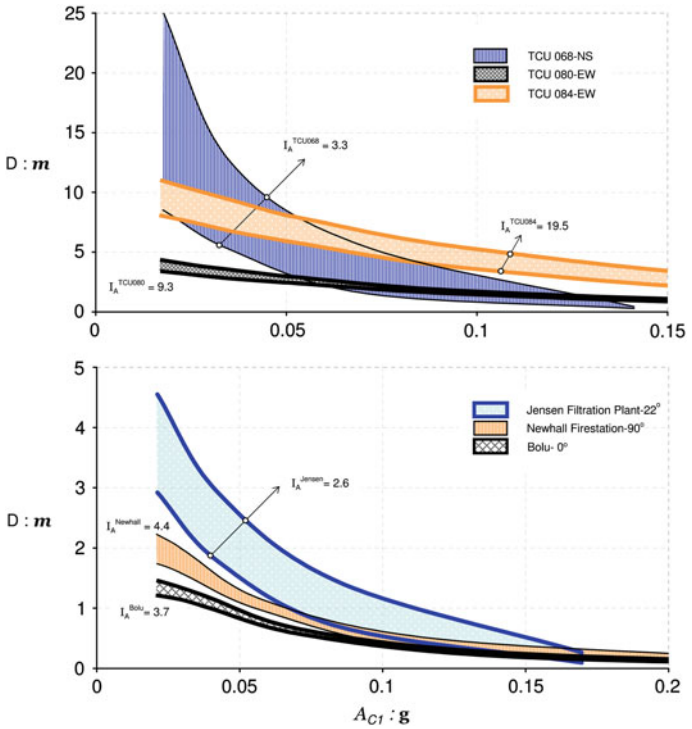

Fig. 14 Induced slippage versus critical acceleration: No convincing correlation could be found between the accumulated slip and the Arias Intensity, I_A, of the records. A "mere" reversal of polarity, while leaving I_A unchanged, may lead to differences by a factor of 3

duration of their motions is vastly different. The FKS 017 and TCG 014 motions last up to 150 s whereas the Takatori record ends after almost 30 s. This fact reflects the magnitude difference between the two earthquakes: the Tohoku event had a magnitude of M = 9 and Kobe M = 7.2.

The frequency content of the motions is also vastly different: Takatori is rich in components with periods ranging from 0.5 to 2.5 seconds; the Tohoku motions are rich only in very low periods, between 0.2 and 0.4 s—a surprising result given their huge magnitude.

Figure 16, first of all, shows that the performance of I_A is far worse for the symmetric system, the results of which are portrayed on the top of figure. The smaller the Arias Intensity the larger the slip of the block! The Takatori record with $I_A = 8.7$ m/s leads to much greater maximum slippage D (by a factor of 4 or 5) in the whole range of yield acceleration values than the TCG 014 motion of $I_A = 20.1$ m/s! With asymmetric sliding (bottom figure) the difference is still in favor of Takatori but not as spectacular (by a factor of about 1.5–2). The reason, of course, is the accumulation of downhill slippage which increases almost in unison with both the number of cycles and Arias Intensity —hence, the Tohoku motions with very high I_A and huge number of cycles are not as benign (although still more benign than Takatori).

Interestingly, the actual differences in the observed damage to buildings from shaking in the two earthquakes (2011 and 1995) are consistent with the above difference in slippage computed for the three motions: much larger in Kobe than in the Tohoku region. The selection of "severe" motions in this paper was of course somewhat arbitrary; still, one can draw a

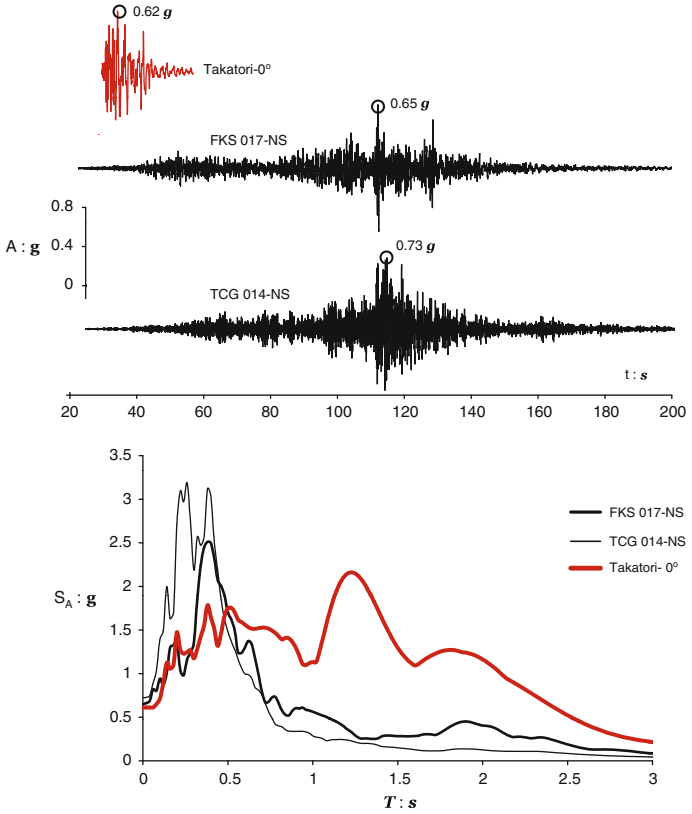

Fig. 15 Acceleration time-histories of three records plotted in the same scale: the FKS 017 and TCG 014 records from the disastrous 2011 Tohoku earthquake and the Takatori ground motion from the 1995 Kobe event. At the *bottom* figure, the elastic response spectra of the three motions (damping 5%)

first conclusion of potential interest: Arias Intensity can not alone be a reliable predictor of damage of a specific ground motion, especially if the latter contains acceleration pulses of large duration (directivity or fling related). However, with the accumulation of a large number of records, it is with no doubt a reasonable parameter for statistical inference.

The above conclusion is in accord with Sarma and Kourkoulis (2004) and Crespellani et al. (1998). The latter, utilised for slope deformation, a corrected measure of motion "destructiveness", denoted P_D, as proposed by Araya & Saragoni and based on Arias Intensity, normalised with a frequency parameter: the average rate of zero-crossing of the record. In this study, P_D proved somewhat superior to I_A.

5.2 Improvement of the Makdisi and Seed charts

We compare the results of this study against the classical relevant charts for sliding published by Makdisi and Seed (1978). In Figs. 17 and 18 are demonstrated our results for the seismic events of magnitude 6.0–6.8 and 6.9–7.7 respectively. Evidently, for small A_{Cl}/A_H values (<0.30) these classical curves, which were obtained by processing a number of (mostly "usual") records available at the time (mainly from the San Fernando 1971 earthquake), can

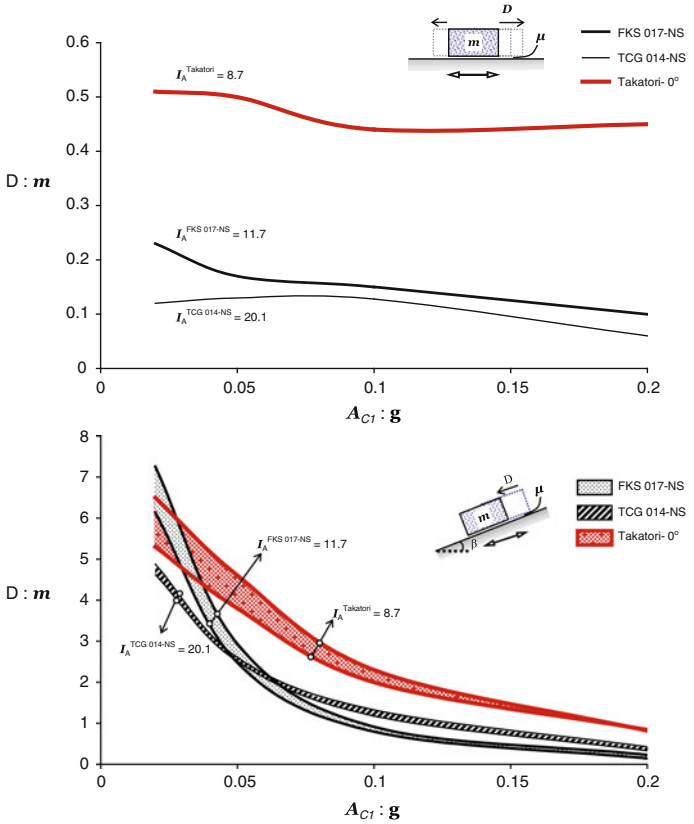

Fig. 16 Slippage induced by the FKS 017, TCG 014 and Takatori records (from the 2011 Tohoku and the 1995 Kobe events) versus the critical acceleration A_{C1}. The top figure corresponds to symmetric sliding (*horizontal sliding plane*) whereas the bottom plot to the asymmetric, one-sided sliding (*inclined sliding plane*). The Arias intensity, I_A, of each record is shown. The correlation between D and I_A is much worse in symmetric sliding

not adequately predict the extreme slippage produced with motions strongly affected by fling and directivity phenomena. Based on our data, admittedly of a rather limited number (2×99), and for A_{C1}/A_H ratio values in the range of [0.05, 0.4] the upper bound of sliding displacements can be estimated with the following two analytical expressions:

$$D = 500 \exp(-7\, A_{C1}/A_H), \quad \text{for} \quad 6.0 < M < 6.8 \tag{14}$$

$$D = 3{,}000 \exp(-10\, A_{C1}/A_H), \quad \text{for} \quad 6.9 < M < 7.7 \tag{15}$$

These expressions can be utilised for a quick assessment of the maximum possible damage from a near-fault "unpredictably" severe ground motion with strong directivity and fling effects. The exponential form of Eqs. (14) and (15) is employed as the regression-fit function with the best correlation index R^2. Note that numerous researchers have also presented their estimation of sliding displacement with respect to critical acceleration ratio in exponential form (Jibson 2007; Cai and Bathurst 1996; Yegian et al. 1991; Ambrasseys and Menu 1988; Whitman and Liao 1984; Richards and Elms 1979; Makdisi and Seed 1978; Franklin and Chang 1977; Sarma 1975).

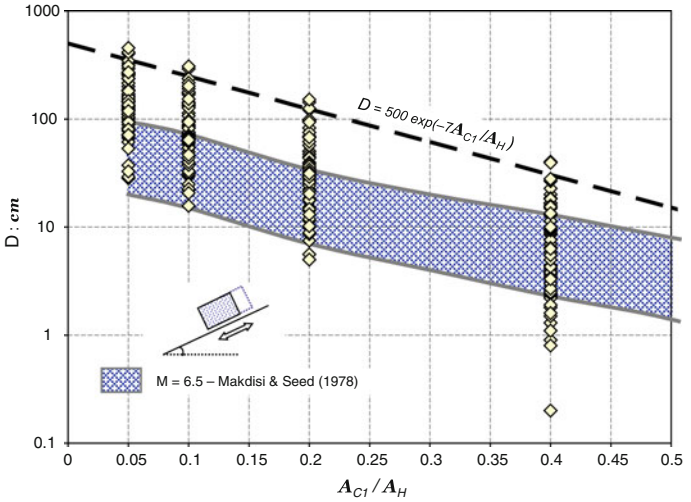

Fig. 17 Comparison of the Makdisi and Seed (1978) curve with the sliding induced by records from earthquake events of magnitude 6.0–6.8. Each excitation is imposed with the + and − polarity. The dashed line represents an effective upper bound of slippage triggered by such strong motions

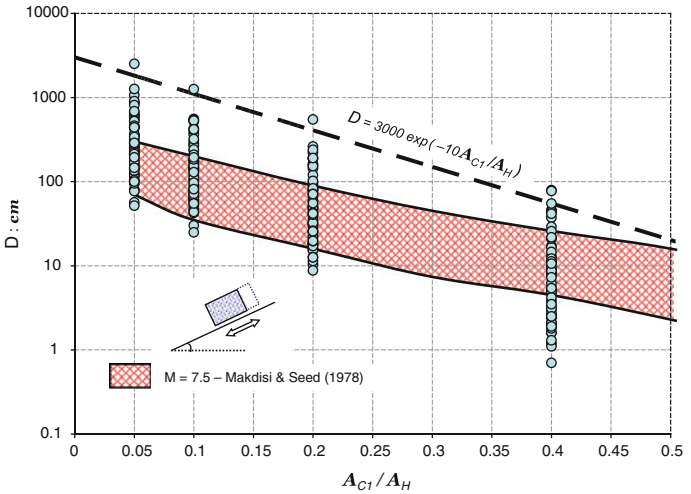

Fig. 18 Comparison of the Makdisi and Seed (1978) curve with the sliding induced by records from earthquake events of magnitude 6.9–7.7. Each excitation is imposed with the + and − polarity. The dashed line represents an effective upper bound of slippage triggered by such strong motions

Conclusions

Using the accumulated slippage of a block resting on inclined plane shaken by an accelerogram as the "damage" inflicted to the system, the paper investigates the possible correlation of this damage with various "Intensity Measures" of the particular accelerogram. "Intensity Measures" (or as named in this paper "Indices of Destructiveness") widely utilised in the literature or developed here are studied with 2 × 99 ground motions recorded in near-fault

conditions in 13 earthquakes. These were not the typical frequently-observed motions but records bearing the signature of forward directivity and fling-step phenomena, to a larger or a smaller degree.

Some of these 'Indices of Destructiveness' are shown to be completely inadequate predictors of the computed damage. Including in this list are PGA, A_{RMS}, I_C, ASI and SMA. A few indices are modestly inadequate. Only I_H, P_D, and I_A show a decent (but far from excellent) correlation and are therefore recommended for application in practice,*but only in a truly statistical sense.* Because as a more detailed deterministic analysis has clearly revealed, the predictive power of one of the statistically successful measures, Arias intensity (I_A), is rather poor for asymmetric sliding. For symmetric sliding, where accumulation of slippage is of little if any significance, anticipating the degree of "damage" on the basis of I_A could be completely misleading—at least for the type of severe ground motions considered herein.

An evaluation of the state-of-practice curves $D = D(A_C/A_H; M)$ of Makdisi and Seed (1978) against the results of this study shows that they underpredict the extreme values of D produced by directivity and fling affected motions. Expressions are given for a "truly" upper-bound estimate of slippage in practice.

Acknowledgments The work outlined in this paper has been conducted within the PERPETUATE Research project, funded by the European Commission's Seventh Framework Programme (FP7/2007–2013) under the grand agreement N° 244229 (www.perpetuate.eu).

References

Abrahamson NA (2000) Effects of rupture directivity on probabilistic seismic hazard analysis. In: Proceedings, 6th international conference on seismic zonation, palm springs, California, Earthquake Engineering Research Institute

Abrahamson NA (2001) Incorporating effects of near fault tectonic deformation into design ground motions. University at Buffalo MCEER: Friedman F.V. Professional Program, webcast: http://mceer:buffalo.edu/outreach/pr/Abrahamson.asp

Alavi B, Krawinkler H (2000) Consideration of near-fault ground motion effects in seismic design. In: Proceedings of the 12th world earthquake conference on earthquake engineering, New Zealand

Ambraseys NN, Menu JM (1988) Earthquake-induced ground displacements. Earthq Eng Struct Dyn 16: 985–1006

Ambraseys NN, Sarma SK (1967) The response of earth dams to strong earthquakes. Géotechnique 17: 181–213

Ambraseys NN, Srbulov M (1994) Attenuation of earthquake-induced ground displacements. Earthq Eng Struct Dyn 23:467–487

Araya R, Saragoni G (1984) Earthquake accelerogram destructiveness potential factor. In: Proceedings of 8th world conference on earthquake engineering, pp 835–842

Arias A (1970) A measure of earthquake intensity, In: Hansen RJ (ed) Seismic design for nuclear power plants. MIT Press, Cambridge, pp 438–483

Bertero VV (1976) Establishment of design earthquakes: evaluation of present methods. In: Proceedings, international symposium of earthquake structural engineering, vol 1, University of Missouri-Rolla, St. Louis, pp 551–580

Bertero VV, Mahin SA, Herrera RA (1978) Aseismic design implications of near-fault san fernando earthquake records. Earthq Eng Struct Dyn 6:31–42

Bray JD, Rathje EM (1998) Earthquake-induced displacements of solid-waste landfills. J Geotech Geoenviron Eng ASCE 124:242–253

Cai Z, Bathurst RJ (1996) Deterministic sliding block methods for estimating seismic displacements of earth structures. Soil Dyn Earthq Eng Elsevier 15:255–268

Changhai Z, Shuang L, Xie LL, Yamin S (2007) Study on inelastic displacement ratio spectra for near-fault pulse-type ground motions. Earthq Eng Eng Vib Springer 6(4):351–356

Constantinou MC, Gazetas G (1987) Probabilistic seismic sliding deformations of earth dams and slopes. In: Proceedings of the specialty conference on probabilistic mechanics and structural reliability, ASCE, pp 318–321
Constantinou MC, Gazetas G, Tadjbakhsh I (1984) Stochastic seismic sliding of rigid mass against asymmetric coulomb friction. Earthq Eng Struct Dyn 12:777–793
Crespellani T, Madiai C, Vannucchi G (1998) Earthquake destructiveness potential factor and slope stability. Geotechnique 48:411–420
Franklin A, Chang FK (1977) Earthquake resistance of earth and rock-fill dams, report 5: permanent displacements of earth embankments by Newmark sliding block analysis. Miscellaneous paper S-71-17, soils and pavements laboratory, U.S. Army Engineer Waterways Experiment Station, Vicksburg
Garini E, Gazetas G (2012) Destructiveness of earthquake ground motions: "Intensity Measures" versus sliding displacement. In: Proceedings of the 2nd international conference on performance-based design in earthquake geotechnical engineering, Taormina, Italy, Paper No. 7.07, pp 886–899
Garini E, Gazetas G, Anastasopoulos I (2011) Asymmetric 'Newmark' sliding caused by motions containing severe 'directivity' and 'fling' pulses. Géotechnique 61(9):733–756
Gazetas G, Garini E, Anastasopoulos I, Georgarakos T (2009) Effects of near–fault ground shaking on sliding systems. J Geotech Geoenviron Eng ASCE 135(12):1906–1921
Gazetas G, Uddin N (1994) Permanent deformation on pre-existing sliding surfaces in dams. J Geotech Eng ASCE 120(11):2041–2061
Gazetas G, Debchaudhury A, Gasparini DA (1981) Random vibration analysis for the seismic response of earth dams. Géotechnique 31(2):261–277
Hall JF, Heaton TH, Halling MW, Wald DJ (1995) Near-source ground motion and its effects on flexible buildings. Earthq Spectra 11(4):569–605
Harp EL, Jibson RW (1995) Seismic instrumentation of landslides: building a better model of dynamic landslide behaviour. Bull Seismol Soc Am 85:93–99
Hisada Y, Bielak J (2003) A theoretical method for computing near-fault ground motions in layered half-spaces considering static offset due to surface faulting, with a physical interpretation of fling step and rupture directivity. Bull Seismol Soc Am 93(3):1154–1168
Housner GW (1952) Spectrum intensities of strong motion earthquakes. In: Proceedings of the symposium on earthquake and blast effects on structures, EERI, Oakland California, pp 20–36
Iwan WD, Huang CT, Guyader AC (2000) Important features of the response of inelastic structures to near-fault ground motion. In: Proceedings of the 12th world earthquake conference on earthquake engineering, New Zealand, Paper No. 1740
Jibson RW (2007) Regression models for estimating coseismic landslide displacement. Eng Geol 91:209–218
Jibson RW (1994) Predicting earthquake-induced landslide displacements using Newmark's sliding block analysis. Transportation Research Record, No. 1411, Transportation Research Board, Washington, DC, pp 9–17
Kramer SL, Lindwall NW (2002) Dimensionality and directionality effects of Newmark stability analysis. J Geotech Geoenviron Eng ASCE 130:303–315
Kramer SL, Smith M (1997) Modified Newmark model for seismic displacements of compliant slopes. J Geotech Geoenviron Engin ASCE 123:635–644
Lagomarsino S, Giovinazzi S (2006) Macroseismic and mechanical models for the vulnerability and damage assessment of current buildings. Bull Earthq Eng 4:415–443
Lin JS, Whitman RV (1983) Decoupling approximation to the evaluation of earthquake-induced plastic slip in earth dams. J Geotech Eng Div ASCE 11:667–678
Ling H (2001) Recent applications of sliding block theory to geotechnical design. Soil Dyn Earthq Eng ASCE 21(3):189–197
Makdisi FI, Seed HB (1978) Simplified procedure For estimating dam and embankment earthquake induced deformations. J Geotech Eng Div ASCE 104:849–867
Makris N, Roussos YS (2000) Rocking response of rigid blocks under near-source ground motions. Géotechnique 50(3):243–262
Makris N, Chang S (2000) Effect of viscous, visco-plastic and friction damping on the response of seismic isolated structures. Earthq Eng Struct Dyn 29:85–107
Mavroeidis PG, Dong G, Papageorgiou SA (2004) Near-fault ground motions, and the response of elastic and inelastic single-degree-Of-freedom (SDOF) systems. Earthq Eng Struct Dyn 33:1023–1049
Nuttli OW (1979) The relation of sustained maximum ground acceleration and velocity to earthquake intensity and magnitude. US Army Engineer Waterways Experiment Station. Miscellaneous Paper S-76-1, Report 16, p 74
Newmark NM (1965) Effects of earthquakes on dams and embankments. Géotechnique 15(2):139–160

Pavlou EA, Constantinou MC (2004) Response of elastic and inelastic structures with damping systems to near-field and soft-soil ground motions. Eng Struct 26:1217–1230
Pitilakis K (2004) Site effects. In: Ansal A (ed) Recent advances in geotechnical engineering and microzonation. Springer, New York, pp 139–197
Richards R, Elms DG (1979) Seismic behaviour of gravity retaining walls. J Geotech Eng Div ASCE 105: 449–464
Richards R, Elms DG, Budhu M (1993) Seismic bearing capacity and settlement of foundations. J Geotech Eng ASCE 119:662–674
Sarma SK (1975) Seismic stability of earth dams and embankments. Géotechnique 2(4):743–761
Sarma SK (1981) Seismic displacement analysis of earth dams. J Geotech Eng Div ASCE 107:1735–1739
Sarma SK, Yang KS (1987) An evaluation of strong motion records and a new parameter A95. Earthq Eng & Struct Dyn 15(1):119–132
Sarma SK, Kourkoulis R (2004) Investigation into the prediction of sliding block displacements in seismic analysis of earth dams. In: Proceedings of the 13th world conference on earthquake engineering, Vancouver, Canada, paper no 1957
Sasani M, Bertero VV (2000) Importance of severe pulse-type ground motions in performance-based engineering: historical and critical review. In: Proceedings of the 12th world conference on earthquake engineering, New Zealand, Paper No 1302
Sawada T, Chen WF, Nomachi SG (1993) Assessment of seismic displacements of slopes. Soil Dyn Earthq Eng 12:357–362
Seed HB, Martin GR (1966) The seismic coefficient in earth dam design. J Soil Mech Found Div ASCE 92:25–58
Seyedi M, Gehl P, Davenne L, Ghavamian S, Mezher N, De Douglas, J., Martin F, Modaressi H (2007) Numerical modelling of the influence of earthquake strong-motion characteristics on the damage level of a reinforced concrete structure. 7ème Colloque National AFPS, Ecole Centrale Paris, ID: A095
Shen J, Tsai MH, Chang KC, Lee GC (2004) Performance of a Seismically Isolated Bridge under Near-Fault Earthquake Ground Motions. Journal of Structural Engineering, ASCE 130:861–868
Singh JP (1985) Earthquake ground motions: implications for designing structures and reconciling structural damage. Earthq Spectra 1:239–270
Somerville P (2000) Seismic hazard evaluation, 12th WCEE 2000. Bull N Z Soc Earthq Eng 33:325–346, 484–491
Somerville PG, Smith NF, Graves RW, Abrahamson NA (1997) Modification of empirical strong ground motion attenuation relations to include the amplitude and duration effects of rupture directivity. Seismol Res Lett 68:199–222
Stamatopoulos CA, Velgaki EG, Modaressi A, Lopez-Caballero F (2006) Seismic displacement of gravity walls by a two-body model. Bull Earthq Eng 4:295–318
Stamatopoulos CA (1996) Sliding system predicting large permanent co-seismic movements of slopes. Earthq Eng Struct Dyn 25:1075–1093
Von Thun JL, Rochim LH, Scott GA, Wilson JA (1988) Earthquake ground motions for design and analysis of dams. Earthquake engineering and soil dynamics II—recent advances in ground-motion evaluation. Geotechnical Special Publication 20, ASCE, pp 463–481
Whitman RV, Liao S (1984) Seismic design of gravity retaining walls. In: Proceedings of the 8th world conference on earthquake engineering, vol 3, San Francisco, pp 533–540
Wartman J, Bray JD, Seed RB (2003) Inclined plane studies of the Newmark sliding block procedure. J Geotech Geo-environ Eng ASCE 129(8):673–684
Xu LJ, Rondriguez-Marek A, Xie LL (2006) Design spectra including effect of rupture directivity in near-fault region. Earthq Eng Eng Vib Springer 5(2):159–170
Yegian MK, Marciano EA, Ghahraman VG (1991) Earthquake induced permanent deformations: a probabilistic approach. J Geotech Eng ASCE 117:35–50
Yegian MK, Harb JN, Kadakal U (1998) Dynamic response analysis procedure for landfills and geosynthetic liners. J Geotech Geoenviron Eng ASCE 124(10):1027–1033